

Thermo-mechanical field-scale testing of a partially activated energy pile in Vienna

Adrian Thylbert Brunner, Roman Markiewicz, Johannes Pistor, Dietmar Adam
Institute of Geotechnics, TU Wien, Austria, adrian.brunner@tuwien.ac.at

ABSTRACT: The City of Vienna and TU Wien have a long history of using and testing energy geostructures as part of ground source heat pump systems. In the framework of a research project, in which numerous foundation elements were tested for their serviceability and load-bearing capacity, two dedicated field-scale energy piles were investigated for the first time in Vienna. The large-bored pile presented here was equipped with a double steel pipe in the upper part for shaft-friction to be limited to the Miocene sediments soil layer consisting of silty fine sands and sandy silt. Furthermore, the heat transfer pipe loops were installed in the lower areas only while being fed through the upper parts of the pile, allowing a concentrated activation of both the pile skin friction and the thermal load in the homogeneous soil layer. The test pile was fully instrumented with strain gauges, extensometers, temperature sensors and optical fibers and tested for nearly three months. The mechanical load, applied as dead load, remained constant during the heating and cooling cycles to isolate the pile responses. In addition to the geomechanical investigation, the pile setup was also used as part of unconventional thermal response tests to establish the thermal parameters of the soil layers and concrete via numerical back-calculations. Finally, the pile was subjected to a conventional static load pile test to determine the ultimate load, enabling comparisons between the energy pile and other conventional large-bored piles close by.

KEYWORDS: Energy piles, thermo-active ground-source systems, field-scale tests, thermo-mechanical behavior.

1 INTRODUCTION

Energy geostructures and especially energy piles have been used successfully in Austria since the 1980's (Brandl, 2006). In the past two decades, several field-scale energy piles have also been scientifically investigated (a summary has been given, e.g., by Cunha, et al. (2022)). However, a comprehensive field-scale study of the thermo-mechanical behavior of these foundation elements in Vienna's ground conditions has been pending for a long time. In 2017, the City of Vienna – Municipal Department 29 for Bridge Construction and Foundation Engineering – and TU Wien conducted a research project to determine the load-bearing behavior of various foundation elements frequently used in Vienna ("Forschungsprojekt Unteres Hausfeld" – FPUH). This allowed two field-scale energy piles with different depths and diameters to be tested, of which one – the so-called "energy pile Miocene" (B.EM) installed in Miocene sediments – is addressed here. More details have been published by Markiewicz, et al. (2024).

Beyond representing the first energy pile tests under Vienna ground conditions, this research introduces several novel aspects to field-scale testing. The investigation employed non-uniform thermal activation, examined partial mobilization of shaft resistance within homogeneous soil layers, and incorporated extensive and redundant monitoring systems. The testing sequence implemented thermo-mechanical cycles over several months followed by a static pile load test to assess both cyclic thermal effects and residual ultimate load capacity. The static pile load tests of identically constructed conventional reference piles (without thermal loading) at the same site enables direct comparison of load-deformation behavior and ultimate bearing capacity.

2 FIELD-SCALE TEST SETUP

2.1 Ground conditions and pile installation

The ground conditions of the test site in the north-east of Vienna are influenced by the Danube River and are typical for large parts of the city. Quaternary sandy gravels are found up to a drilling depth of about 10 m, with the natural groundwater table close to the surface at approx. 2 m depth. Below this, Miocene deposits in the form of silty fine sands to clayey silts are found. The ground conditions derived from nearby rotary core drillings are shown in Figure 1.

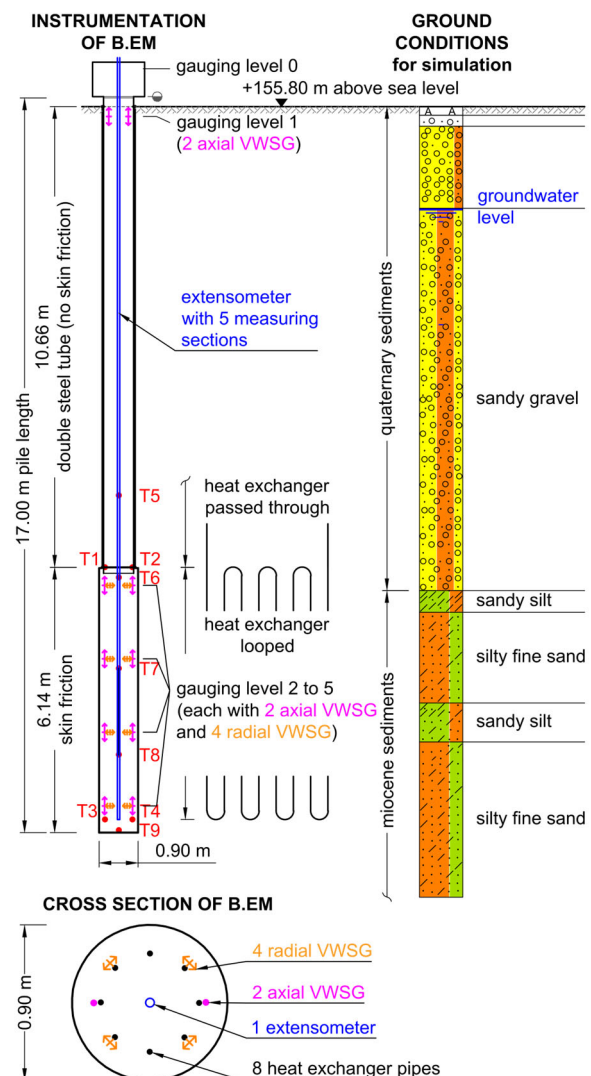


Figure 1. Schematic longitudinal section and cross section of the test pile with instrumentation and installation position of the heat exchanger pipes and ground conditions derived from nearby rotary core drillings.

The energy pile was bored with a diameter of 0.9 m and a total length of 17 m, extending to 17.8 m including the pile cap. To ensure that shaft friction is only mobilized in the Miocene sediments, the Quaternary layer was bridged using a double steel tube. The heat exchanger pipes were looped for a total of eight cross-sections in the lower part of the energy pile and simply passed through the upper part, effectively concentrating the thermal loads in the pile sections with shaft friction (see Figure 1).

2.2 Instrumentation

The test pile was extensively equipped with various measuring instruments to record the load deformation behavior of the pile on the one hand and the temperature conditions of the pile on the other hand (see Figure 1). The pile head was equipped with a load cell and vertical and horizontal displacement transducers. In the energy pile itself, vibrating wire strain gauges (VWSG) measured axial strains, radial strains and temperatures in different cross-sections. Optical fiber sensing was additionally employed for redundant, high-resolution strain and temperature measurements, with a further aim of comparing the performance of different measurement systems. Furthermore, an extensometer was placed in the pile center to measure deformations, and several temperature gauges (T1 to T9 in Figure 1) were placed throughout the pile. In addition to the instrumentation inside the pile, thermal wire cables (TIP) were installed in three nearby boreholes to capture the temperature conditions in the ground. Finally, temperatures in the reaction piles, the outer air temperature, inlet and outlet heat exchanger fluid temperatures as well as the flow rate were measured. It should be noted that not all available sensors were evaluated for this work.

2.3 Test procedure

The test procedure was derived by numerically modelling the energy pile using a three-dimensional, time dependent thermal simulation with COMSOL Multiphysics in advance (Markiewicz, et al., 2024). The testing was finally carried out for 78 days in total in several phases, as shown in Figure 2a. In phase 0, a dead load up to 1 MN was applied on the pile head by stacking concrete blocks on the loading platform. This approach was critical to avoid load fluctuations as well as power supply backups for the hydraulic press (Bourne-Webb, et al., 2009). In the following phases 1 to 4 the mechanical load was kept constant at 0.6 MN resp. 0.8 MN, with load cycles to 1 MN performed at the end of the first two phases. Additionally, thermal loading was applied via the heat exchanger pipes by setting the inlet temperatures to 35 °C and 2 °C for heating and cooling, respectively (Figure 2b). The difference between the inlet and outlet temperature was limited to 2 K. Phase 5 served as preparation for a conventional static pile load test and for regeneration towards natural temperature conditions in order to uncouple the effects of the mechanical and thermal loading, as suggested by Bourne-Webb, et al. (2009). Finally, in phase 6 the energy pile was tested until failure using a hydraulic press, almost exhausting the maximal capacity of 6 MN.

3 MEASUREMENT RESULTS

3.1 Temperature

Figure 2b shows the temperature load (curve “inflow”) applied by the heat exchanger pipes as well as the temperatures of the pile and in the nearby boreholes at gauge level 3 (see Figure 1). The latter shows that the temperature effect decays very rapidly near the energy pile in the Miocene soil layer. At a distance of 1.75 m from the pile axis the temperature influence is already negligible. These results are in excellent agreement with the

numerical simulation in COMSOL Multiphysics (Markiewicz, et al., 2024), which also showed that an extension of the heating or cooling periods would have caused only minor changes. Furthermore, the measurements are very similar to those in the London Clay (Bourne-Webb, et al., 2009).

In Figure 3a, the temperature differences between the beginning and end of heating phase 3 and cooling phase 4 are plotted along the pile length for both the vibrating wire strain gauges (VWSG) and the optical fiber sensor (OFS). The results show good agreement between the two measurement systems. However, due to the positioning of the heat exchanger loops in the lower part of the pile, the thermal loads, and consequently the temperature differences, are not uniformly distributed along the pile length. This highlights an advantage of the OFS over the VWSG, as it enables a more detailed analysis of the temperature distribution.

3.2 Load-displacement behavior

Figure 2c shows the pile-head response due to mechanical and thermal loading. The settlements of the initial loading in phase 0 are followed by a greater amount of uplift in the first heating phase. The subsequent cooling and heating cycles show pile-head movements of similar magnitudes to each other. It can generally be observed that the temperature loads of 35 °C and 2 °C for heating and cooling, respectively, have a greater influence on the pile-head displacement than the mechanical load of 1 MN. Both thermal and mechanical loads were chosen to represent typical serviceability conditions.

The pile exhibited different settlement behavior due to mechanical load cycles between heating and cooling phases, likely due to changes in pile-soil contact conditions. While some studies suggest that radial thermal expansion has a minimal effect on contact stresses (Faizal, et al., 2019), this will be further investigated using available radial strain data.

To evaluate the pile head displacements in relation to theoretically free thermal expansion, a methodology from Bourne-Webb, Bodas Freitas and Freitas Assunção (2019) was adapted and applied to the discussed energy pile by Markiewicz, et al. (2024). Due to the non-uniform thermal loading along the pile, free expansion was calculated by integrating OFS temperature data over the pile length. This allowed the determination of theoretical free expansion values and the corresponding ratios of measured to theoretically free displacement (z_0/z_{Free}), from which the location of the neutral point H_n , i.e., the point at which the shaft resistance reverses, could be inferred. The results show an upward shift of the neutral point during early heating phases, suggesting higher shaft resistance relative to base resistance. With continued thermo-mechanical cycling, z_0/z_{Free} ratios approached 1.0, indicating increasing contribution from the pile base. These trends, along with observed settlement behavior, suggest possible long-term changes in load transfer mechanisms due to cyclic thermal loading. A more detailed analysis, including model assumptions and implications for design, is presented by Markiewicz, et al. (2024).

In the recovery phase 5, the settlements decreased upon removing the mechanical and thermal load, but the initial level was not reached again. In phase 6 during the pile load test, the mechanical load was increased to 5.4 MN with a pile head displacement of 163 mm, which returned to 154 mm after unloading (see Section 3.4).

3.3 Axial strain

The strain ϵ_{M-Obs} during the exclusively mechanical loading in phase 0 in Figure 3b shows a slight decrease in strains from the pile-head (gauging level 1) to the bottom of the double steel pipe (gauging level 2), possibly due to the double steel tube not

being completely frictionless, or inaccuracies in the evaluation due to different degrees of reinforcement or stiffness. In greater depths the strain diminishes completely up to the pile foot, which leads to the assumption that the load is exclusively transferred into the ground via shaft friction in phase 0.

Figure 3b also shows the range between axial strain due to completely free expansion and radially restrained expansion. The measured temperature-related axial strains ϵ_{T-Obs} lie between these cases. Both were calculated with a typical coefficient of thermal expansion of $\alpha_c = 10 \mu\epsilon/K$, which might be too low for the given pile. In any case, the strains ϵ_{T-Obs} were approximately in the order of the (theoretical) free strains ϵ_{T-Free} . It can therefore be concluded that the energy pile was able to expand almost freely and that the thermal load led to deformations that correspond to the (theoretical) deformations with free boundary conditions. The almost free temperature-related deformation behavior of the energy pile can also be concluded from the measured pile head deformations (Section 3.2) as well as from the small stress related strains ϵ_σ (Figure 2d). It can also be concluded that a mechanical load many times higher than 1 MN would have been necessary to

prevent axial expansion in the heating case (Markiewicz, et al., 2024).

3.4 Pile load test and ultimate load

The static pile load test (Figure 4), which was carried out on the energy pile in phase 6, can be compared to a conventional pile with the same properties only 35 m away. The energy pile thereby shows favorable load-settlement behavior as well as a higher ultimate load of 5.4 MN compared to 4.1 MN of the reference pile. Additionally, the energy pile exhibited a final pile head displacement 18 mm smaller than the conventional pile (163 mm vs. 181 mm). This might be caused by the additional thermal preloading, which anticipated settlements and created better contact between the pile and the soil (especially in the area of the pile base). However, another contributing factor might be some variation in soil properties.

Finally, after the end of the pile load test the heat absorber pipes of the energy pile were inspected for damage and none was found despite the large deformations.

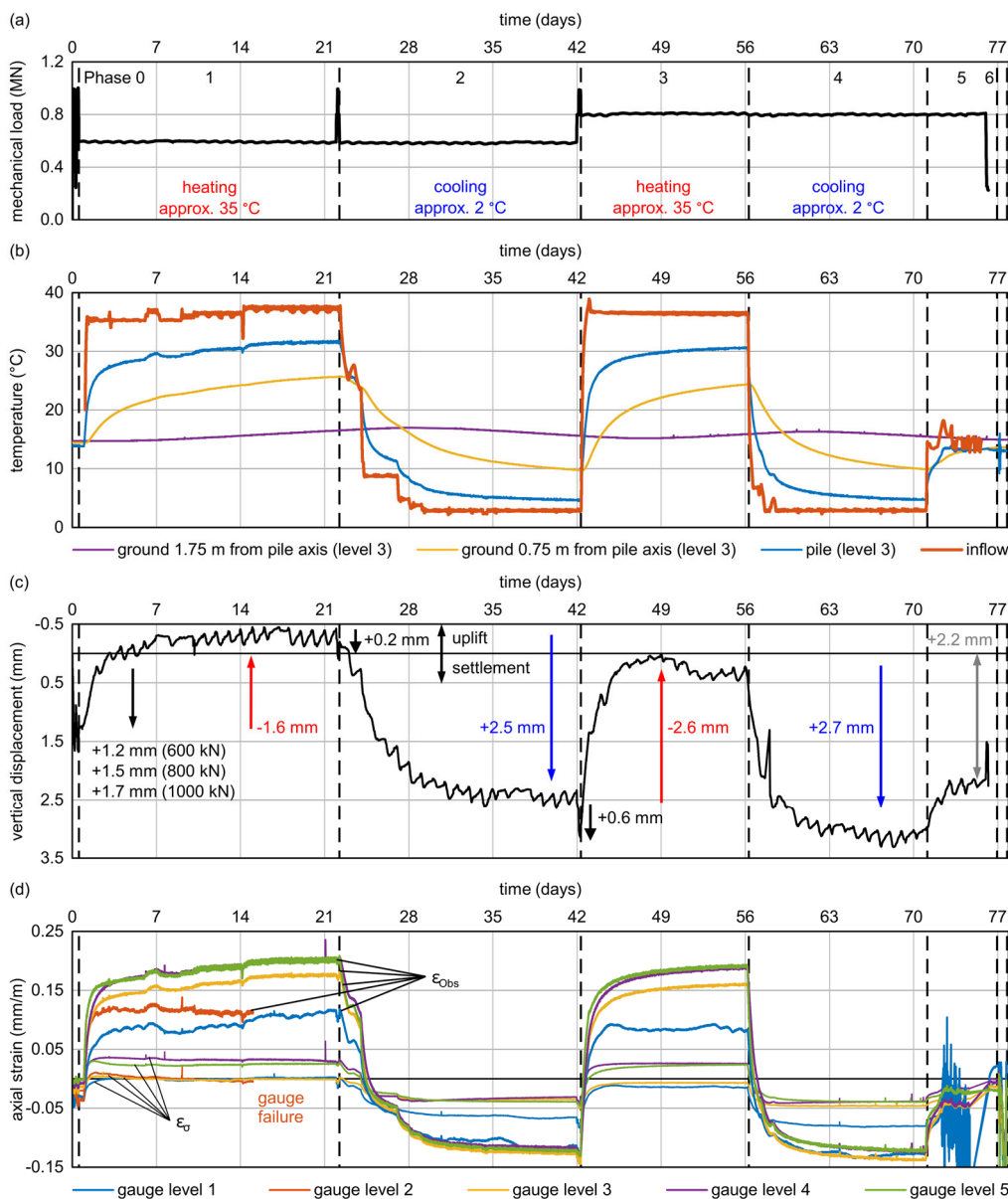


Figure 2. Measurement results: (a) mechanical dead load in the phases 0 to 5; (b) thermal load applied with heat exchanger pipes and temperatures in gauge level 3 in and near the pile; (c) vertical pile head displacement; (d) axial strain components.

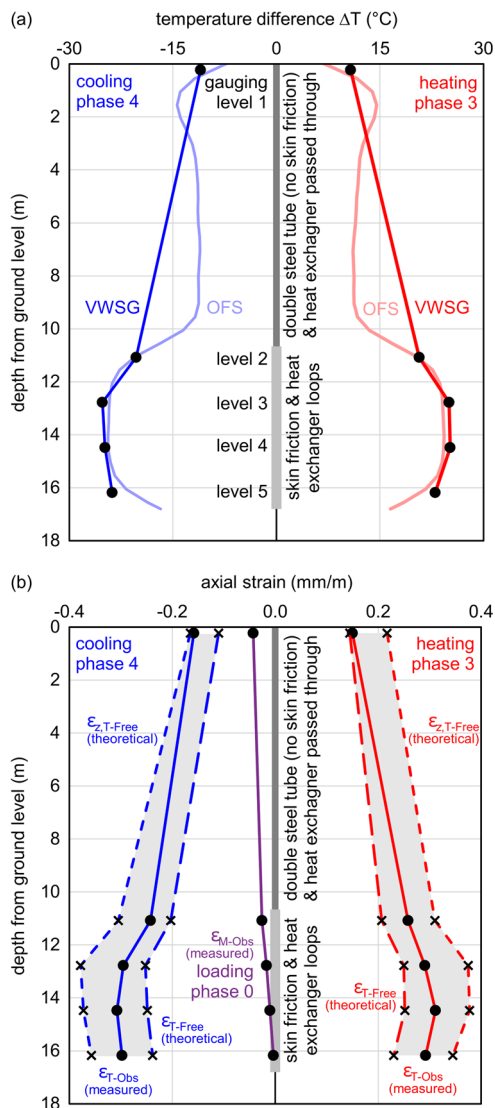


Figure 3. Measurement results: (a) temperature difference between beginning and end of heating resp. cooling phase measured with optical fiber sensors (OFS) and vibrating wire strain gauges (VWSG); (b) measured axial strain components due to mechanical loading (ϵ_{M-Obs} due to 800 kN) and due to thermal loading (ϵ_{T-Obs} due to ΔT) as well as theoretical free strains (ϵ_{T-Free} due to ΔT).

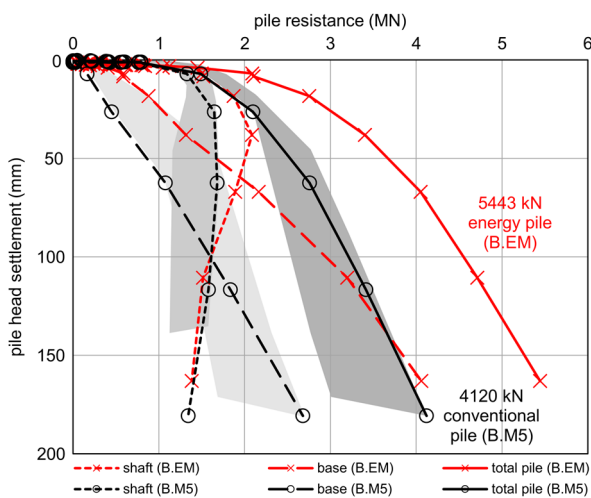


Figure 4. Results of static pile load tests: B.EM (energy pile); B.M5 (conventional pile with same diameter and length); the shaded areas show the envelopes of all five conventional piles B.M1 to B.M5.

4 SUMMARY AND OUTLOOK

Energy geostructures have been used to heat and cool buildings for decades with no incidents of damage known to the authors. Nevertheless, the structural response of these elements to combined mechanical and thermal loading is of scientific and practical interest to ensure a safe and economic design.

This study presents results from the first field-scale energy pile tests conducted in Vienna. The methodological innovations of this field-scale test advance understanding of energy pile behavior under realistic operational conditions and provide data for energy pile design in Vienna and similar geological environments.

Temperature data showed excellent agreement with numerical simulations, confirming that thermal effects of energy pile operation remain highly localized within the Miocene soil layer, with ground temperature differences rapidly decreasing with distance from the pile axis. Under representative service conditions, thermal loads exerted greater influence on pile-head displacements than mechanical loads. The energy pile deformed almost freely, as evidenced by small stress-related strain components compared to observed strains, resulting in low additional stresses, as well as other measurements. Analysis of strain distribution revealed that the mechanical load alone was transferred exclusively via shaft friction in the Miocene layer, while the pile base resistance was likely activated with progressive thermal load cycles. Comparison with nearby conventional piles revealed that the energy pile exhibited favorable load-displacement behavior, with a greater ultimate load capacity, while showing lower settlements. Post-testing inspection confirmed no damage to the heat exchanger system despite loading to ultimate capacity.

5 ACKNOWLEDGEMENTS

The authors gratefully acknowledge the City of Vienna – Municipal Department 29 for Bridge Construction and Foundation Engineering – for financial and technical support of this project.

6 REFERENCES

- Bourne-Webb, P.J., Amatya, B., Soga, K., Amis, T., Davidson, C. and Payne, P., 2009. Energy pile test at Lambeth College, London: geotechnical and thermodynamic aspects of pile response to heat cycles. *Géotechnique*, 59(3), pp.237–248. <https://doi.org/10.1680/geot.2009.59.3.237>.
- Bourne-Webb, P.J., Bodas Freitas, T.M. and Freitas Assunção, R.M., 2019. A review of pile-soil interactions in isolated, thermally-activated piles. *Computers and Geotechnics*, 108, pp.61–74. <https://doi.org/10.1016/j.compgeo.2018.12.008>.
- Brandl, H., 2006. Energy foundations and other thermo-active ground structures. *Géotechnique*, 56(2), pp.81–122. <https://doi.org/10.1680/geot.2006.56.2.81>.
- Cunha, R.P. and Bourne-Webb, P.J., 2022. A critical review on the current knowledge of geothermal energy piles to sustainably climatize buildings. *Renewable and Sustainable Energy Reviews*, 158. <https://doi.org/10.1016/j.rser.2022.112072>.
- Faizal, M., Bouazza, A., McCartney, J.S. and Haberfield, C., 2019. Axial and radial thermal responses of energy pile under six storey residential building. *Canadian Geotechnical Journal*, 56(7), pp.1019–1033. <https://doi.org/10.1139/cgj-2018-0246>.
- Markiewicz, R., Brunner, A.T., Pistol, J. and Adam, D., 2024. Field investigations on the thermo-mechanical behavior of a partially activated energy pile in Miocene sediments. *Geomechanics for Energy and the Environment*, [online] 40. <https://doi.org/10.1016/j.gete.2024.100605>.